Astron. Astrophys. 354, 247–252 (2000)

ASTRONOMY AND ASTROPHYSICS

Evidence for dust emission in the Warm Ionised Medium using WHAM data

G. Lagache[1], L.M. Haffner[2], R.J. Reynolds[2], and S.L. Tufte[3]

[1] Institut d'Astrophysique Spatial, Bât. 121, Université Paris XI, 91405 Orsay Cedex, France
[2] University of Wisconsin, Astronomy Department, Madison, WI 53706, USA
[3] Lewis & Clark College, Department of Physics, Portland, OR 97219, USA

Received 26 August 1999 / Accepted 19 November 1999

Abstract. We have used the WHAM H_α survey and Leiden/Dwingeloo HI data to decompose the Far-infrared emission (from 100 to 1000 μm) at high Galactic latitude into components associated with the Warm Ionised Medium (WIM) and the Warm Neutral Medium (WNM). This decomposition is possible for the first time thanks to preliminary WHAM data that cover a significant fraction of the sky (about 10%). We confirm the first detection of dust emission from the WIM (Lagache et al. 1999) and show that the WIM dust temperature and emissivity are very similar to those in the WNM. The analysis suggests moreover that about 25% of the far-IR dust emission at high Galactic latitude is uncorrelated with the HI gas. The decomposition again reveals a Cosmic Far-Infrared Background (CFIRB) which is determined for the first time from 100 to 1000 μm using two independent gas tracers.

Key words: ISM: dust, extinction – infrared: ISM: continuum – ISM: general

1. Introduction

Two discoveries have recently opened new perspectives on the understanding dust evolution in the Warm Ionised Medium (WIM). Howk & Savage (1999) have pointed out, for the first time, the existence of Al- and Fe-bearing dust grains towards two high-z stars. They have shown that the degree of grain destruction in the ionised medium through these two stars is not much higher than in the warm neutral medium. In addition, Lagache et al. (1999) have for the first time detected the infrared dust emission associated with the WIM based on FIRAS data analysis. This study reveals a dust emissivity in the WIM which does not differ much from that of the HI gas. However, the detection of infrared emission from dust in the WIM is difficult because one can not easily separate the contribution of the H^+ gas from that of the HI gas. For the first time, the WHAM H_α sky survey of our Galaxy ($\delta > -30^o$) offers the unique opportunity to separate the dust emission associated with the diffuse H^+ and HI gas. Measuring and characterising the dust emission from the WIM could allow to understand the evolution of the dust grains in the low-density gas. Moreover, dust grain can play an important role in heating the diffuse ionised gas (through the photoelectric effect, Reynolds & Cox, 1992) and can be responsible at least in part of forbidden line strengths (Sembach et al. in press; Bland-Hawthorn et al. 1997).

Dust emission associated with the HI gas has been extensively studied using the spatial correlation between the infrared dust emission and the 21 cm HI emission. Boulanger et al. (1996) using DIRBE and FIRAS data together with the HI emission as measured by the Leiden/Dwingeloo survey of the northern hemisphere have found that the dust emission spectrum derived from this correlation can be quite well represented by a single modified Planck curve characterized by T=17.5 K and $\tau/N_{HI} = 10^{-25}\ (\lambda/250\,\mu\mathrm{m})^{-2}$ cm^2. This emissivity law is very close to the one predicted by the Draine & Lee (1984) dust model.

Studies of the far-infrared emission at high Galactic latitude have also revealed a residual component interpreted as the Cosmic Far-InfraRed Background (Puget et al. 1996; Fixsen et al. 1998; Hauser et al. 1998; Lagache et al. 1999). This background is produced by the line of sight accumulation of all extragalactic objects that are not resolved in the FIRAS or DIRBE beam. Cosmological implications derived from this background can be found for example in Dwek et al. (1998) and Gispert et al. submitted.

In this paper, we present a decomposition of the far-infrared sky emission using the HI Leiden/Dwingeloo (Hartmann & Burton, 1997) and the WHAM H_α surveys (Reynolds et al. 1998). This decomposition gives new determinations of the dust emission associated with the diffuse HI and H^+ gas as well as the CFIRB. Our study is limited to very diffuse regions. Detail comparisons between HI, H_α and far-infrared filaments are beyond the scope of this paper and will be adressed in future works.

The paper is organised as follows. First (Sect. 2), we present the data we have used. Sect. 3 describes the regions selected for the decomposition as well as the decomposition method. We then present the results (Sect. 4). Finally, a summary is given in Sect. 5.

Send offprint requests to: lagache@ias.fr

2. Data presentation

2.1. Far-infrared and HI data

We have used far-infared data from the DIRBE and FIRAS instruments on board the COBE satellite. The FIRAS instrument is a polarising Michelson interferometer with 7° resolution and two separate bands (from 2.2 to 20 cm^{-1} and from 20 to 96 cm^{-1}) which have a fixed spectral resolution of 0.57 cm^{-1} (Fixsen et al. 1994). The study presented here is based on "pass 4" data which have been corrected for the zodiacal light (Kelsall et al. 1998), the Cosmic Microwave Background and its dipole emission (see the FIRAS explanatory supplement). DIRBE is a photometer with ten bands covering the range from 1.25 to 240 μm with 40 arcmin resolution (Silverberg et al. 1993). We only use the last three bands (100, 140 and 240 μm) for which the zodiacal emission has been subtracted. These maps are called "Zodi-Subtracted Mission Average Maps"[1].

We decide in our analysis to work at the FIRAS resolution (1) to increase the DIRBE map signal to noise ratio and (2) to combine FIRAS and DIRBE data. Thus, we convolve the DIRBE maps with the FIRAS Point Spread Function (PSF). The PSF is not precisely known for all wavelengths, so we use the approximation suggested by Mather (private communication) of a 7° diameter circle convolved with a line of 3° length perpendicular to the ecliptic plane (Mather et al. 1986).

The HI data we used are those of the Leiden/Dwingeloo survey which covers the entire sky down to $\delta = -30°$ with a grid spacing of 30' in both l and b. The 36' half power beam width of the Dwingeloo 25 - m telescope provides 21 - cm maps at an angular resolution which closely matches that of the DIRBE maps. Details of the observations and correction procedures are given by Hartmann (1994) and by Hartmann & Burton (1997). The 21cm-HI data are convolved with the FIRAS PSF. We derive the HI column densities using 1 K km s^{-1}=1.82 10^{18} H cm^{-2} (optically thin emission).

2.2. WHAM data

The WHAM[2] Sky Survey provides the first northern hemisphere, velocity-resolved map of H_α from our Galaxy ($\delta > -30^o$). The WHAM instrument is a Fabry-Perot spectrometer which uses a low noise, high efficiency CCD camera as a detector behind a pair of 15 cm diameter Fabry-Perots. WHAM provides a 12 km s^{-1} velocity resolution with one-degree angular resolution down to sensitivity limits of 0.2 R (1 R = $10^6/4\pi$ ph cm^{-2} s^{-1} sr^{-1}) in a 30 second exposure. The one-degree angular resolution nicely matches the DIRBE resolution and allows direct comparison between these two datasets. We have used two parts of the WHAM survey centred on (l,b)=(148^o, -20^o) and (l,b)=(138^o, 36^o). The two maps ($40^o \times 50^o$ and $60^o \times 20^o$ respectively) are called map1 and map2. For these two regions, preliminary data reduction has been done including bias subtraction, reflected ring subtraction, annular-summing and flat-fielding. The geocoronal H_α line is easily removed due to the velocity separation between this atmospheric emission line and the Galactic emission line. A first-order polynomial fits the sky background well within the WHAM 200 km s^{-1} bandpass. The typical level of the subtracted background is about 0.03-0.07 R $(km\ s^{-1})^{-1}$. Some spectra in the direction of stars brighter than the sixth magnitude contain the H_α absorption line from the star. These pointings appear as isolated 1^o diameter depression in the otherwise smooth emission at high Galactic latitude. Intensity calibration is performed using frequent observations of nebular sources. All WHAM intensities are tied to the absolute intensity measurement of the North American Nebula (NGC 7000). The uncertainty on the H_α emission for this preliminary dataset is about 10%. Details on WHAM can be found in Tufte (1997), Haffner (1999) and Reynolds et al. (1998).

For comparison with COBE data, WHAM data have been first projected on the DIRBE sixcube. A 5×5 pixel median filtering has been applied in order to remove the defects induced by stellar H_α absorption lines from several lines of sight. These data are then convolved with the FIRAS beam.

3. Decomposition of the far-infrared emission

3.1. Pixel selection

The decomposition of the far-infrared emission in very diffuse regions requires careful selection of pixels on the sky mainly to avoid HII regions and IR emission from molecular clouds. We apply several criteria:

– We remove pixels with $|\beta| < 10^o$ to avoid any contamination by residual zodiacal emission.

– Only high Galactic latitude regions are selected (b lower than -30^o and greater than 25^o for map1 and map2 respectively).

– Diffuse parts of the sky are selected following Lagache et al. (1998). To remove molecular clouds and HII regions, we use the DIRBE map of the 240 μm excess with respect to the 60 μm emission: $\Delta S = S_\nu(240) - 4 \times S_\nu(60)$. This map shows as positive flux regions, the cold component of the dust emission, and as negative flux regions, regions where the dust is locally heated by nearby stars (like the HII regions). Therefore, diffuse emission pixels are selected with $|\Delta S| < 3\sigma$, σ being evaluated from the width of the histogram of ΔS (the distribution of ΔS is gaussian with a "negative" and "positive" wing corresponding to heated dust regions and cold molecular clouds respectively). This criteria is for example important for the map2 where it removes the cold Polaris, Ursa major and Camelopardalis clouds. It removes 6.4% of the original high ecliptic and galactic latitude maps.

– We keep all regions for which the Hα emission is between 0.2 and 2 R. The lower value (0.2 R) ensures that we are well above the noise. The threshold of 2 R is arbitrary but ensures that the remaining pixels are not coming from bright enhanced Hα regions caused by an increase of the electron density.

– Pixels with high HI column densities (N(HI) > 6 10^{20} H cm^{-2}) are removed. We use this HI threshold rather than that derived in Boulanger et al. (1996) and Lagache et al. (1999)

[1] DIRBE and FIRAS data are available on the Web site http://www.gsfc.nasa.gov/astro/cobe

[2] WHAM informations can be found on the Web site http://www.astro.wisc.edu/wham

since it increases the statistics by 30%. With such a criterium, the contribution of the cold dust emission is lower than 3% in the far-infrared bands.

We keep 122 FIRAS pixels, corresponding to 2% of the sky.

3.2. Conversion of the WHAM H_α intensity into N(H^+)

IR emission that can be correlated with the ionised gas cannot be simply related to this gas phase as for the HI component. Emission from HI gas is proportional to N(HI), whereas WIM emission is derived from the emission measure which is proportional to n_e^2 (where n_e is the WIM electron density). Thus, the WIM intensity measured in Rayleighs, considering a constant electron density along the line of sight, is proportional to $N(H^+)n_e$. For a WIM dust temperature of T_e=8000 K, we compute a conversion factor (from Osterbrock, 1989):

$$I_\alpha(R) = 14.5 \times n_e \times N(H^+)_{20cm^{-2}} \quad (1)$$

where $N(H^+)_{20cm^{-2}}$ is the H^+ column density normalised at 10^{20} H cm^{-2}. This conversion factor depends weakly on the temperature. We see from Eq. (1) that it is impossible to disentangle if variations in I_α are due to variations in the electron density or variations in the H^+ column density.

For our sample, the mean H_α intensity is equal to 0.69 R with a standard deviation of 0.37 R. For the case where H_α intensity variations are only due to variations in n_e with a constant H^+ column density, we can estimate the infered electron densities. For our selected pixels, the minimal and maximal H_α intensity is equal to 0.2 R and 1.9 R respectively. This gives a variation in the electron density by a factor of $\sim$10. Such a variation is not expected in our very diffuse high galactic latitude regions averaged in the FIRAS 7^o beam. This is supported by the study of Reynolds (1991) who has derived for the mean electron density $\langle n_e \rangle$=0.08 cm^{-3} along high latitude sightlines a dispersion of 0.04 cm^{-3}. Thus we conclude that most of the H_α intensity variations in the data used for this study are due to variations in H^+ column density rather than in n_e. Using $\langle n_e \rangle$=0.08 $\pm$ 0.04 cm^{-3}, we compute from Eq. (1) the following conversion factor[3]:

$$I_\alpha(R) = 1.15 \pm 0.6 \times N(H^+)_{20cm^{-2}} \quad (2)$$

3.3. Decomposition method

Using the conversion factor derived in the previous section, we can describe the far-infrared dust emission as a function of the HI and H^+ column density by:

$$IR = A \times N(HI)_{20cm^{-2}} + B \times N(H^+)_{20cm^{-2}} + C \quad (3)$$

where N(HI)$_{20cm^{-2}}$ and N(H^+)$_{20cm^{-2}}$ are the column densities normalised at 10^{20} H cm^{-2}. The coefficients A, B and the constant term C are determined simultaneously using regression fits. Before performing the infrared regression analysis, we have correlated the HI with the H^+ gas. The correlation coefficient between these emission lines is about 38% for the selected pixels. Such a weak correlation may come from the cosecant variation of the two components. Removing the cosecant variations before the analysis results in a correlation coefficient of zero.

At DIRBE wavelengths the fit has been done using a relative weight computed from the standard deviation maps. The statistics uncertainty on A and B coefficients are very small compared to real variations of A and B across the sky. However, we do not yet have enough statistics to test their spatial variations which will be done using the complete WHAM survey.

The A, B and C values obtained using different weights for the fit are very consistent. Only their statistical uncertainties change significantly. As we have checked that A, B and C coefficients do not vary with different weights for DIRBE, the fit has been done using the same weight for each pixel at the FIRAS wavelengths.

The uncertainty in the conversion factor (Eq. (2)) do not affect the determination of the A and C coefficients. It only changes the normalisation of B.

Before computing the regression fit analysis, we should have removed the cosecant law variations for each of the components: dust, HI and H^+. However, due to small statistics ($\sim$ 2% of the sky), it is very difficult to accuratly derive the slopes of these relationships. We have checked using DIRBE data at 100, 140 and 240 μm (at the 7^o resolution) that the results derived by removing the best estimate of the cosecant variations before the fit are in good agreement with ones obtained without this correction. Thus, we conclude that for our small dataset, the cosecant law variations do not affect the result of the decomposition.

4. Results and discussion

This section presents the results obtained for A, B and C and compares them with previous determinations. The A coefficient is the spectrum of the dust associated with HI gas for N(HI)=10^{20} H cm^{-2}; if detected, B will give the dust emission spectrum associated with the ionised gas for N(H^+)=10^{20} H cm^{-2}; and C is the residual Cosmic Far-InfraRed Background.

4.1. Spectrum of the dust associated with HI gas

The spectrum of the dust associated with HI gas (the A coefficient computed at each FIRAS wavelength) is shown on Fig. 1. It is limited to $\lambda >$180 μm due to the very low signal to noise ratio of FIRAS data at shorter wavelengths. Also reported are A values obtained at the DIRBE wavelengths (and given in Table 1). We see a very good agreement between the spectrum obtained from the decomposition and the one derived by Lagache et al. (1999). To determine the temperature and emissivity of the dust in HI gas, we fit the FIRAS spectrum by a ν^2 modified Planck curve. We obtain a temperature of 17.2 K with an emissivity:

$$\tau/N(HI) = 8.3 \quad 10^{-26}(\lambda/250\,\mu\mathrm{m})^{-2} \quad cm^2 \quad (4)$$

[3] We can also derive using our H_α intensity dataset the dispersion for $\langle n_e \rangle$ by considering that the H^+ column density is constant, and assigning H_α intensity variations to variations in $\langle n_e \rangle$. We obtain the same dispersion of 0.04 cm^{-3}.

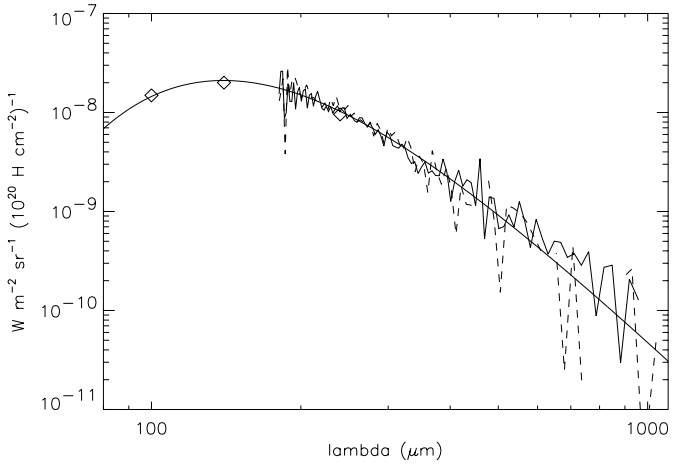

Fig. 1. Dust emission spectrum associated with HI gas for N(HI)=10^{20} H cm^{-2}. The dashed and continuous lines represent the spectrum derived in Lagache et al. (1999) and the result of the decomposition (A coefficient) respectively. Also reported are the DIRBE values at 100, 140 and 240 μm (diamonds), as well as a ν^2 modified Planck curve with a temperature of 17.2 K. Errors on the DIRBE points are smaller than the symbol.

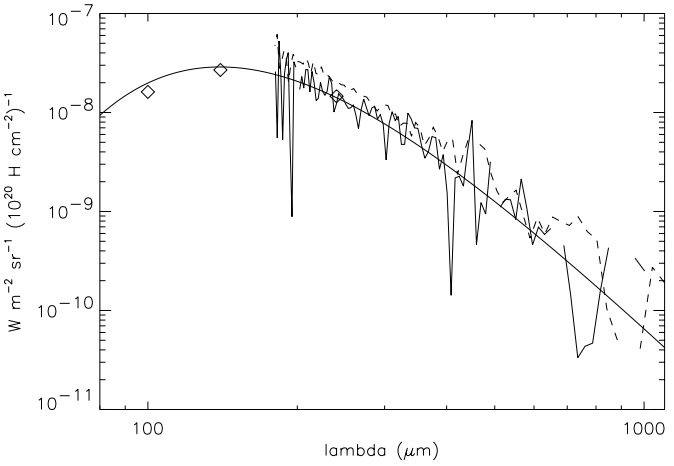

Fig. 2. Dust emission spectrum associated with the ionised gas for N(H^+)=10^{20} H cm^{-2}. The dashed and continuous lines represent the spectrum derived in Lagache et al. (1999) and the result of the decomposition (B coefficient) respectively. Also reported are the DIRBE values at 100, 140 and 240 μm (diamonds), as well as a ν^2 modified Planck curve with a temperature of 17.2 K. Errors on the DIRBE points are smaller than the symbol

Table 1. DIRBE dust emission associated with HI (A) and H^+ (B) gas for N(HI)=10^{20} H cm^{-2} and N(H^+)=10^{20} H cm^{-2} respectively, and CFIRB (C) at 100, 140 and 240 μm. Errors on A and B are statistical. On the CFIRB, errors have been estimated using the width of residual emission ($IR - A \times N(HI) - B \times N(H^+)$) histograms (statistical errors are negligible).

λ	A MJy/sr/10^{20}	B MJy/sr/10^{20}	C MJy/sr
100	0.50±0.004	0.54±0.016	0.78±0.21
140	0.93±0.027	1.26±0.103	1.13±0.54
240	0.77±0.021	1.17±0.078	0.88±0.55

This emissivity law is very close to the one predicted by the Draine & Lee (1984) dust model as was also shown previously by Boulanger et al. (1996). The relative uncertainty on the emissivity computed by keeping the modified 17.2 K Planck curve inside the statistical errors is about 10%.

4.2. Spectrum of the dust associated with the WIM

The B coefficient reveals a spectrum which is clearly non-zero (Fig. 2). This spectrum, although much more noisy, is in very good agreement with the previous determination made on a larger fraction of the sky (25.6%, Lagache et al, 1999). This confirms without ambiguity the first detection of the WIM dust emission.

The level of the spectrum derived here is 1.3 times lower than the previous one. This factor comes from (1) the use of the new DIRBE and FIRAS data (for the maps used in Lagache et al. 1999, the correction of the zodiacal emission was not as accurate as for the corrected maps delivered by the DIRBE and FIRAS team) and (2) the difference in the normalisation. Compared to the previous result, DIRBE data points (Table 1) show a decrease of the spectrum at short wavelengths, suggesting a dust temperature smaller than in the previous study. This decrease was not seen before in the FIRAS spectrum due to the very low signal to noise ratio below 180 μm. However, the spectrum given by the B coefficient is too noisy to determine the dust temperature accuratly. The range of temperature allowed by the spectrum is between 16 and 18 K. In Fig. 2 is displayed, for direct comparison with the HI gas dust emission a ν^2 modified Planck curve with a temperature of 17.2 K. With this temperature, the emissivity of the dust in the ionised gas is:

$$\tau/N(H^+) = 1.1 \quad 10^{-25}(\lambda/250\,\mu\mathrm{m})^{-2} \quad cm^2 \tag{5}$$

The relative uncertainty on the emissivity computed by keeping the modified 17.2 K Planck curve inside the statistical errors is about 10%. There is no doubt that dust emission associated with the WIM is detected. However, the uncertainty on the conversion factor (Eq. (2)) induces a possible error on the emissivity value of about 50%.

The dust emissivity in the WIM derived for $\langle n_e \rangle$=0.08 cm^{-3} is very close to the one derived in the HI gas, which confirms a dust abundance in the WIM that does not differ much from that of the HI gas. Such a conclusion is in very good agreement with the recent work of Howk & Savage (1999). With their absorption-line studies of the WIM of the Galaxy, they provide evidence for dust in the diffuse ionised gas. Their analysis implies that the processing of dust grains in the WIM may not be much different than that in the HI gas. The similar temperature and emissivity of dust in HI and H^+ gas support this conclusion. The temperature and emissivity of the dust in the ionised gas will be more accuratly determined using the whole WHAM survey.

These results can be compared with the study of Arendt et al. (1998) which uses a similar method in order to find the far-

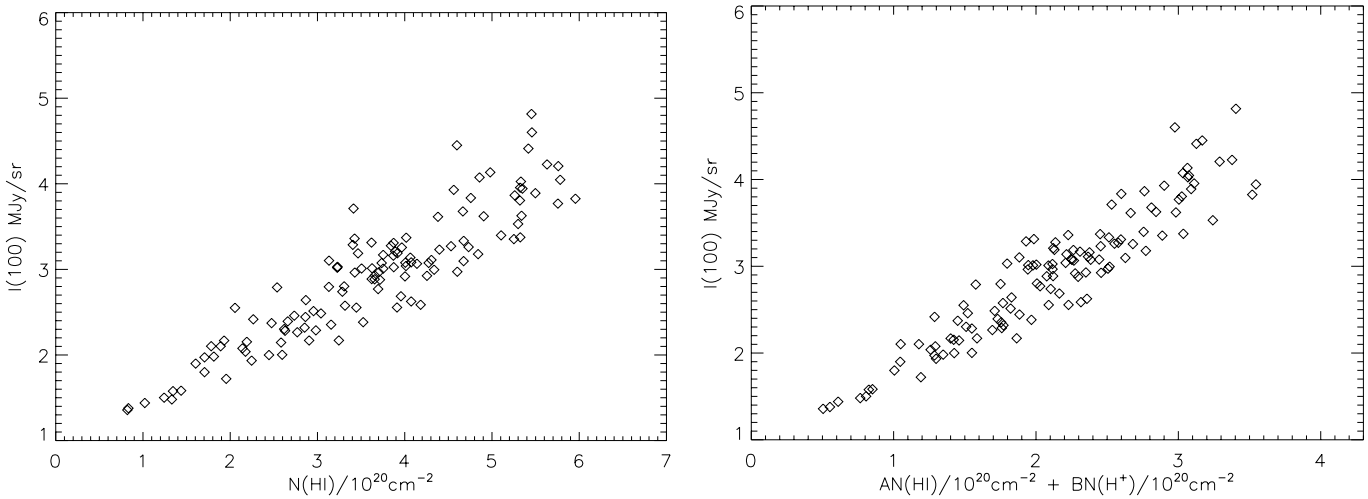

a **b**

Fig. 3. **a** Correlation between the 100 μm DIRBE emission and the HI column density (normalised at 10^{20} H cm^{-2}). **b** correlation between the 100 μm emission and the result of the decomposition $A \times N(HI)_{20cm^{-2}} + B \times N(H^+)_{20cm^{-2}}$

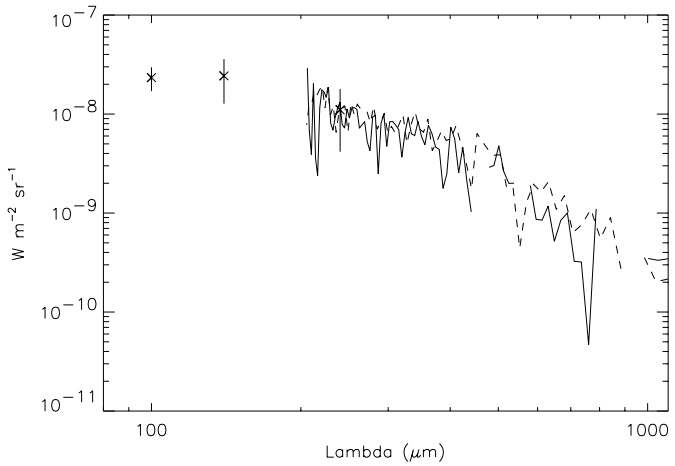

Fig. 4. CFIRB spectra obtained from the decomposition of the far-infrared sky (continuous line) and determined on the Lockman Hole region (dashed line) by Lagache at al. (1999). Also reported are DIRBE values at 100, 140 and 240 μm.

infrared emissivity of the diffuse ionised gas. They conclude that they were unable to detect any IR emission associated with low density ionised gas at high Galactic latitude. This non-detection can be easily explained by the very small fraction of the sky that was used (the largest region represents about 0.2% of the sky).

Heiles et al. (1999) have done exactly the same decomposition (Eq. (3)) at 100 μm in the Eridanus superbubble except that they have used for the infrared emission at 100 μm the temperature-corrected DIRBE data from Schlegel et al. (1998). This region is much more complicated than the diffuse parts of the sky selected here and the value of B varies significantly from region to region. This variation likely reflects the variation of n_e from 0.62 to 1.2 cm^{-3} (Heiles et al. 1999). These electron densities are much higher than that in the WIM (which is about 0.08 cm^{-3}). The mean B value obtained by Heiles et al. (1999) is 0.84 MJy/sr/10^{20} H cm^{-2} which is only a factor 1.5 above our determination, which may be surprising considering the difference in the physical conditions between our selected parts of the sky and the Eridanus Superbubble.

Fig. 3 shows a comparison beetween the 100μm / HI and 100μm / [AN(HI)+BN(H^+)] correlations. We clearly see the effect of the dust emission associated with the ionised gas. The correlation coefficient is higher using the two gas components rather than using only the HI component (93.6% compared to 91.2%). Combined with the value of the WNM and WIM dust emissivity and assuming that N(H^+)/N(HI)$\sim$25%, this analysis suggests that a significant fraction (about 20-30 %) of the far-IR dust emission at high galactic latitude is uncorrelated with the HI gas.

4.3. The cosmic far-infrared background

The C spectrum obtained by the far-infrared emission decomposition is shown in Fig. 4 together with the CFIRB determination of Lagache et al. (1999) in the Lockman Hole region. We see a very good agreement between the two spectra. These determinations are also in good agreement with the Fixsen et al. (1998) one. This confirmation of the level and shape of the CFIRB supports the validity of the decomposition using the two independent datasets since the constant term in Eq. (3) is very dependent on the determination of A and B.

At 140 and 240 μm, the values obtained for the CFIRB are 1.13$\pm$0.54 MJy/sr and 0.88$\pm$0.55 MJy/sr respectively (Table 1). For each selected pixel, we compute the residual emission, R = IR - A$\times$N(HI) - B$\times$N(H^+). Uncertainties of the CFIRB have been derived from the width of the histogram of R (statistical uncertainties derived from the regression analysis are negligible). The obtained CFIRB values, although much more noisy (due to the small fraction of the sky used), are in very good agreement with Hauser et al. (1998) determinations and the La-

gache et al. (1999) one at 240 μm. At 140 μm, the CFIRB value of Lagache et al. (1999) is smaller than that derived here since the assumed WIM dust spectrum were overestimated (the WIM dust spectrum was very noisy below 200 μm and the estimated dust temperature was too high).

At 100 μm, DIRBE data are less noisy than at 140 and 240 μm (the detector at 100 μm is a photoconductor rather than bolometers at 140 and 240 μm). Assuming an accurate subtraction of the zodiacal emission at this wavelength, our decomposition gives the CFIRB at 100 μm: $I_{CFIRB}(100)$= 0.78$\pm$0.21 MJy/sr. This value can be compared to the non-isotropic residual emission found by Hauser et al. (1998). The average on three regions of the residual emission, equal to 0.73$\pm$0.20 MJy/sr, is in very good agreement with our determination.

5. Summary

We have performed a decomposition of the far-infrared sky at high Galactic latitude using two independent gas tracers: the Leiden/Dwingeloo HI and WHAM Hα surveys of the northern hemisphere of our Galaxy. Main results of this analysis are:

1) The dust emission associated with the HI gas is very well represented by a ν^2 modified Planck curve with a temperature of 17.2 K and an emissivity:

$$\tau/N(HI) = 8.3 \quad 10^{-26}(\lambda/250\,\mu\mathrm{m})^{-2} \quad cm^2$$

This emissivity is in very good agreement with previous determinations (Lagache et al. 1999; Boulanger et al. 1996) and also with the Draine & Lee (1984) dust model.

2) We confirm the first detection of dust emission from the WIM. Assuming a temperature of 17.2 K, the WIM dust emissivity is:

$$\tau/N(HI) = 1.1 \quad 10^{-25}(\lambda/250\,\mu\mathrm{m})^{-2} \quad cm^2$$

suggesting a dust abundance in the WIM comparable to that in the HI gas.

3) The CFIRB obtained from this decomposition is in very good agreement with the previous determinations (Fixsen et al. 1998; Hauser et al. 1998; Lagache et al. 1999). This is the first time that two independent gas tracers for the HI and the H^+ have been used to determine the background at 100 μm: I_{CFIRB}=0.78$\pm$0.21 MJy/sr.

The complete WHAM survey will allow an extension of this decomposition to the whole northern sky. In particular, variation of the dust emission spectrum associated with different ionisation environments will give unprecedent information on the dust processing in the ionised gas of our Galaxy.

Acknowledgements. G.L. is very grateful to R. Reynolds, M. Haffner and S. Tufte for hospitality extended during the stay at the Wisconsin University and for providing early WHAM survey data. Many thanks to David Leisawitz for "pass 4" FIRAS data and to A. Abergel, F. Boulanger and J.L. Puget for their careful reading of the manuscript. WHAM is supported by a grant from the National Science Foundation.

References

Arendt R.G., Odegard N., Weiland J.L., et al., 1998, ApJ 508, 74
Boulanger F., Abergel A., Bernard J.P., et al., 1996, A&A 312, 256
Bland-Hawthorn J., Freeman K.C., Quinn P.J., 1997, ApJ 490, 143
Draine B.T., Lee H.M., 1984, ApJ 285, 89
Dwek E., Arendt R.G., Hauser M.G., et al., 1998, ApJ 508, 106
Fixsen D.J., Cheng E.S, Cottingham D.A., et al., 1994, ApJ 420, 457
Fixsen D.J., Dwek E., Mather J.C., et al., 1998, ApJ 508, 123
Haffner L.M., Reynolds R.J., Tufte S.L., 1998, ApJ 501, L83
Haffner L.M., 1999, Ph.D. Thesis, University of Wisconsin
Hartmann D., 1994, Ph.D. Thesis, University of Leiden
Hartmann D., Burton W.B., 1997, Atlas of Galactic neutral Hydrogen. Cambridge University Press
Hauser M.G., Arendt R.G., Kelsall T., et al., 1998, ApJ 508, 25
Heiles C., Haffner L.M., Reynolds R.J., 1999, In: Taylor A.R., Landecker T.L., Joncas G. (eds.) New Perspectives on the Interstellar Medium. ASP Conference Series Vol. 168
Howk J.C., Savage B.D., 1999, ApJ 517, 746
Kelsall T., Weiland J.L., Franz B.A., et al., 1998, ApJ 508, 44
Lagache G., Abergel A., Boulanger F., Puget J.L., 1998, A&A 333, 709
Lagache G., Abergel A., Boulanger F., et al., 1999, A&A 344, 322
Mather J.C., Toral M., Hemmati H., 1986, Appl. Opt. 25, 16
Osterbrock D.E, 1989, Astrophysics of Gaseous Nebulae and Active Galactic Nuclei. University Science Book
Puget J.L., Abergel A., Bernard J.P., et al., 1996, A&A 308, L5
Reynolds R.J., 1991, ApJ 372, L17
Reynolds R.J., Cox D.P., 1992, ApJ 400, L33
Reynolds R.J., Tufte S.L., Haffner L.M., et al., 1998, PASA 15, 14
Sembach K.R., Howk J.C., Ryans R.S.I., Keenan F.P., ApJ in press
Schlegel D.J., Finkbeiner D.P., Davis M., 1998, ApJ 500, 525
Silverberg R.F., et al., 1993, In: SPIE Conference Proc. 2019 on: Infrared Spaceborne Remote Sensing. San Diego
Tufte S.L, 1997, Ph.D. Thesis, University of Wisconsin